

# EFFICIENTLLM: UNIFIED PRUNING-AWARE PRETRAINING FOR AUTO-DESIGNED EDGE LANGUAGE MODELS

006 **Anonymous authors**

007 Paper under double-blind review

## ABSTRACT

013 Modern large language models (LLMs) driven by scaling laws achieve emergent  
 014 intelligence in large model sizes. Recently, the increasing concerns about cloud  
 015 costs, latency and privacy make it an urgent requirement to develop compact edge  
 016 language models. Distinguished from direct pretraining that bounded by the scal-  
 017 ing law, this work proposes the pruning-aware pretraining, focusing on retaining  
 018 performance of much larger optimized models. It features following characteristics:  
 019 1) Data-Scalable Pruning: we introduce minimal parameter groups in LLM and  
 020 continuously optimize structural pruning, extending post-training pruning methods  
 021 like LLM-Pruner and SparseGPT into the pretraining phase. 2) Auto-Designed  
 022 Architecture: the LLM architecture is auto-designed using saliency-driven prun-  
 023 ing, which is the first time to exceed SoTA human-designed LLMs in modern  
 024 pretraining. We reveal that it achieves top-quality edge language models, termed  
 025 EfficientLLM, by scaling up LLM compression and extending its boundary. Effi-  
 026 cientLLM significantly outperforms SoTA baselines with  $100M \sim 1B$  parameters,  
 027 such as MobileLLM, SmoLLM, Qwen2.5-0.5B, OLMo-1B, Llama3.2-1B in com-  
 028 mon sense benchmarks. As the first attempt, EfficientLLM bridges the performance  
 029 gap between traditional LLM compression and direct pretraining methods, and we  
 030 fully open source EfficientLLM for future advancements.

## 1 INTRODUCTION

031 Large Language Models (LLMs) have become a central component of modern AI systems (Achiam  
 032 et al., 2023; Guo et al., 2025) and are increasingly transforming daily life, particularly in mobile  
 033 edge applications. However, typical LLMs (Touvron et al., 2023a), with 7 billion to 1 trillion  
 034 parameters, require on-cloud deployment and continuous internet connectivity for interface. This  
 035 places significant challenges in terms of latency, data-security and cloud-costs. In fact, fully relying  
 036 on LLMs for mobile edge applications can be impractical — serving all mobile applications with  
 037 GPT-4 (Achiam et al., 2023) would require approximately one million H100 GPUs (Liu et al., 2024b).  
 038 As a result, developing edge language models on resource-constrained devices becomes a recent  
 039 tendency. For instance, MobileLLM (Liu et al., 2024b) focuses on sub-one billion model sizes, which  
 040 would fit in the DRAM of smartphones without excessive consumption.

041 Direct pretraining is dominant in recent tiny language model pretraining. Some practices such as  
 042 MobileLLM and PanGu- $\pi$ -Pro (Tang et al., 2024) design deep-and-thin architectures for model  
 043 efficiency. Other practices such as TinyLlama (Zhang et al., 2024a) and Qwen2.5-0.5B (Yang et al.,  
 044 2024b) focus on scaling up pretraining data to 3T and 17T tokens. Based on best architectures and  
 045 sufficient data, modern tiny models (Yang et al., 2024b; Groeneveld et al., 2024) are showing promise  
 046 in reaching performance boundary. However, their overall performance appears to be somewhat  
 047 locked by the parameter scaling law (Kaplan et al., 2020): given limited model size, simply scaling  
 048 up pretraining data is inefficient. More importantly, the emergent intelligence (Brown et al., 2020) is  
 049 only observed on larger model sizes, meaning tiny models may never achieve this by direct pretraining  
 050 alone. What is the next to train more efficient edge models remains an open challenge.

051 In parallel, LLM compression (Ashkboos et al., 2024; Gu et al., 2024; Han et al., 2015) focus on  
 052 retaining the performance of larger and stronger models while reducing computational cost. Despite

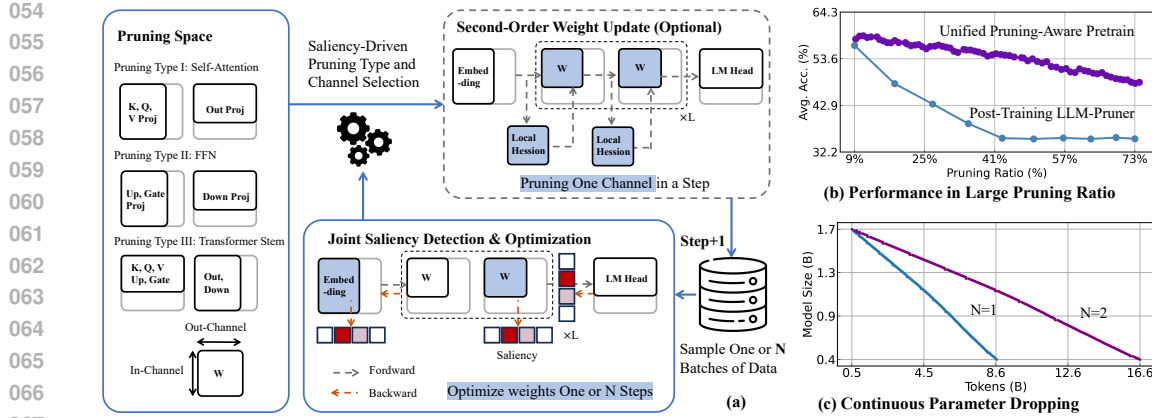


Figure 1: An overview of unified pruning-aware pretraining. (a) Towards **unified pruning, pre-training, and architecture design**, the training loop includes: joint saliency detection and weight optimizing, pruning type selection from pruning space, and weight updating. (b) Improve post-training pruning by pruning-aware pretraining. (c) Continuous model compression during pretraining.

its potential efficiency, existing methods (Sreenivas et al., 2024; Frantar & Alistarh, 2023; Xiao et al., 2023) compress LLM only using a small calibration dataset in post-training, which often results in significant performance degradation, making them unsuitable for top-quality edge language models. Recently, ShearedLlama (Xia et al., 2023) initializes from an optimized LLM, improving training efficiency. However, the constrained optimization (Platt & Barr, 1987) hinders scaling up pruning stage and the performance gap to direct pretraining still remains. This work extends the performance boundary of traditional LLM compression by scaling up training data, a crucial but underexplored approach in the LLM compression field.

This work proposes the unified pruning-aware pretraining to extend the efficiency boundary of edge language models. A family of top-efficiency edge language models in  $100M \sim 1B$  sizes are pretrained, named EfficientLLM. As shown in Fig. 1, we formulate pruning-aware pretraining as a unified framework for weight pruning, pretraining, and architecture design: 1) Compared with direct pretraining, pruning-aware pretraining leverages the performance of much larger optimized models, which direct pretraining smaller models never achieves. 2) Compared with post-training pruning, it scales up the pruning stage with pretraining data. As shown in Fig. 1 (b), pruning-aware pretraining scales up vanilla LLM-Pruner, achieving more than a 10% increase in accuracy. 3) Driven by saliency, the overall architecture can be auto-designed (Yu et al., 2020; Zoph et al., 2018) according to a predefined pruning space step by step.

This work advances both edge language models and LLM compression:

- We propose a family of SoTA edge language models in  $100M \sim 1B$  sizes, named EfficientLLM. EfficientLLM significantly exceeds direct pretrained tiny models by unified and scalable pruning.
- We propose the unified pruning-aware pretraining, promoting LLM compression to the era of pretraining. General post-training methods like LLM-Pruner (Ma et al., 2023), SparseGPT (Frantar & Alistarh, 2023), and Wanda (Sun et al., 2023) could be embedded. By scaling up the pruning stage, vanilla LLM-Pruner significantly exceeds SoTA methods without bells and whistles.
- We explore the auto-designed architectures in modern pretraining for the first time. Saliency-driven architectures are auto-searched via unified pruning and competitive with human practices.

## 2 PRELIMINARY AND RELATED WORKS

**Edge Language Models.** Modern large language models follow the scaling law (Kaplan et al., 2020): larger models achieve higher data efficiency, making optimal training favor large models with moderate data. Towards accurate compact models, a lot of efforts explore the optimal training recipes: 1) data scale. OLMo-1B (Groeneveld et al., 2024), TinyLlama-1.1B (Zhang et al., 2024a), Qwen2.5-0.5B (Yang et al., 2024b) pretrain on 2T, 3T, and 17T tokens respectively, which is significantly larger than the optimal data sizes according to scaling law. 2) Architectures. MobileLLM (Liu et al.,

2024b) shows that the deep-and-thin network and layer sharing achieve additional performance gains. However, direct pretraining is bounded by the scaling law, and can be data-inefficient. More recently, Llama3.2 (Dubey et al., 2024) and MiniTron (Sreenivas et al., 2024) introduce distillation and pruning for data-efficient training. There are mainly 2 drawbacks which addressed in this work: 1) The LLM pruning itself does not scale up. MiniTron only uses a small calibration dataset for pruning and only scales up recovery training, while this work scales up pruning itself to retain more performance. 2) Knowledge distillation (Gu et al., 2024; Ko et al., 2024) during pretraining is not training-efficient, as teacher models are typically 7B-scale LLMs (Touvron et al., 2023b), consuming  $7 \sim 50$ x FLOPs than sub-billion edge models, which we avoid in EfficientLLM. For deployments, quantization (Shao et al., 2023; Xiao et al., 2023; Liu et al., 2024a) can also be adopted.

**LLM Pruning** (Dong et al., 2024; Zhang et al., 2024b; Zhao et al., 2024; Bhaskar et al., 2024). We mainly focus on structural pruning to address hardware friendly edge language models. The most widely used LLM pruning is based on the Taylor expansion (LeCun et al., 1989; Hassibi et al., 1993; van der Ouderaa et al., 2023). By calibration, typical SparseGPT (Frantar & Alistarh, 2023) and Wanda (Sun et al., 2023) can only applied in semi-structured pruning; LLM-Pruner (Ma et al., 2023) only achieves 20% pruning ratio with reasonable accuracy. Even if pruning with finetuning, LoraPrune (Zhang et al., 2023a) can only prune in 50% ratio. So there is an urgent requirement to scale up LLM pruning in pretraining. Another line of works learn to initialize from source model such as ShearedLlama (Xia et al., 2023) and NutePrune (Li et al., 2024) with less than 0.5B tokens. However, ShearedLlama needs human-designed target and does not explore scalability in large scale data; and this work explore unified pruning-aware pretraining with Taylor expansion.

### 3 UNIFIED PRUNING-AWARE PRETRAINING

According to scaling laws, both the scale of training data and the number of parameters are fundamental to the emergence of intelligence in modern LLMs. Direct pretraining of smaller models is inefficient and lacks generalization ability. Model compression methods, although based on pretrained large models, fail to meet the data scale requirements and suffer from significant performance drop.

The principle of this work is to bridge the gap between direct pretraining and LLM compression by a unified training scheme. In practice, pruning-aware pretraining continuously drops parameters in training, which integrates pruning, pretraining, and architecture design at the same time.

**Problem Formulation.** Finding a sub-network from a pretrained LLM is non-trivial. Given an optimized LLM, post-training LLM pruning focuses on finding optimal channels in each layer towards a target architecture. However, for edge language models, it is still challenging to define the efficient target architecture from its source model. For instance, MobileLLM shows the deeper architecture is better than the wider for sub-billion LLMs by human design and practice. However, this best practice may be sub-optimal for a given source model, as each model may exhibit unique saliency patterns that suggest different pruning targets. We formulate the architecture-agnostic pruning problem as:

$$\min_{a \in \mathcal{A}} \min_{c \in \mathcal{C}} \min_w \mathcal{L}_{\text{pretrain}}(a, c, w | \mathcal{M}), \quad (1)$$

where  $\mathcal{A}$  and  $\mathcal{C}$  are sub-architectures (Wu et al., 2019; Liu et al., 2018) and sub-channels sampled from the source model  $\mathcal{M}$ . We jointly optimize pretraining loss through three factors: 1) the sub-architecture,  $a$ , 2) the sub-channels,  $c$ , and 3) the model weights,  $w$ . We outline the pruning-aware pretraining in Fig. 1 and detail each part in the following subsections.

#### 3.1 DEFINING MINIMAL PRUNING GROUP

To design architectures automatically via pruning, we first define the minimal parameter groups as the minimal unit to prune in each step, which should be flexible enough to construct any shape transformers after pruning. Given a pretrained source model  $\mathcal{M}$ , the pruned model  $\mathcal{M}^*$  can be:

$$\mathcal{M}^* = \mathcal{M} - \sum_{t=1}^n g_t, \quad \text{s.t.} \quad \min_{g_t \in \mathcal{G}} \mathcal{L}_{\text{pretrain}}(\mathcal{M}), \quad (2)$$

where  $g_t$  is the mini-group of parameters pruned in step  $t$ , and  $\mathcal{G}$  is the pruning space formulated by defined mini-groups. According to Eq. 2, the pruning can be approximately decoupled by  $t$  steps and

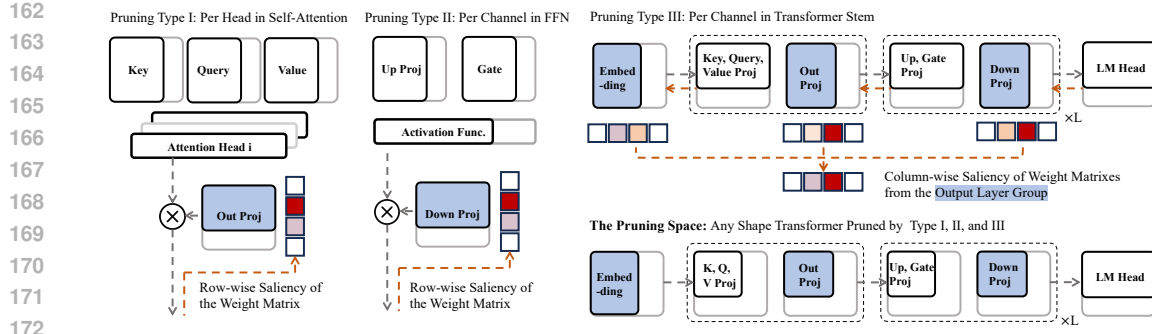


Figure 2: Three basic pruning types in the pruning space. We plot all the weight metrics with shape  $[D_{input}, D_{output}]$ . In backpropagation (in orange), the saliency of the output layer group (in blue) is calculated according to Eq. 9.

solved sequentially:

$$\mathcal{M}_t = \mathcal{M}_{t-1} - g_t^* \quad \text{s.t.} \quad g_t^* = \underset{g_t \in \mathcal{G}}{\operatorname{argmin}} \mathcal{L}_{pretrain}(g_t | \mathcal{M}_{t-1}). \quad (3)$$

We first assume an optimal  $g_t^*$  in each pruning step to minimize pretraining loss, and solve how to acquire  $g_t^*$  in the next subsection. In each pruning step, an optimal mini-group of parameters are selected and dropped from the pretraining LLM  $\mathcal{M}_{t-1}$ , allowing the source model  $\mathcal{M}$  to adaptively reduce the number of parameters until a specific computation budget is met.

For the fully structured pruning space, we impose two constraints in the design of mini-groups: 1) the hidden size, attention heads and intermediate size can be pruned flexibly; 2) the shape of different layers is the same. Unlike LLM-Pruner pruning space, which relies on manually specified pruning targets, our approach divides the pruned parameters into different types of minimal groups that can be adaptively combined during pretraining.

**Parameter Mini-Groups.** For simplify, we indicate the **input layer group** as the *query, key, value projections* in attention blocks; or the *up, gate projections* in feed forward blocks. We indicate the **output layer group** as the *output projections* in attention blocks; or the *down projections* in feed forward blocks. As shown in Fig. 2, we define three basic pruning types and their mini-groups,  $\mathcal{G}_{attn}$ ,  $\mathcal{G}_{ffn}$ ,  $\mathcal{G}_{stem}$ :

1) Per-head pruning in self-attention blocks: when an attention head is pruned, all the corresponding output channels in the input layer group and input channels in the output layer group are pruned at the same time. We select the mini-group  $\mathcal{G}_{attn}^{(\ell)}$  with the minimal saliency in the  $\ell$ th layer, and merge  $\mathcal{G}_{attn}^{(\ell)}$  in all layers as  $\mathcal{G}_{attn}$ :

$$\mathcal{G}_{attn} = \{W_{:,i,:}^{(k,\ell)}, W_{:,i,:}^{(q,\ell)}, W_{:,i,:}^{(v,\ell)}, W_{i,:}^{(o,\ell)}, \ell = 1, 2, \dots, n\}, \quad (4)$$

where  $W_{:,i,:}$  and  $W_{i,:}$  are column-wise and row-wise pruned;  $i$ : $j$  corresponds to channels of an attention head; and  $n$  is the overall blocks.

2) Per-channel pruning in feed-forward blocks: when a intermediate channel is pruned, the coupled channels include one output channel in the input layer group, and one input channel in the output layer group in. We couple the minimal-salinity group  $\mathcal{G}_{ffn}^{(\ell)}$  in the  $\ell$ th layer and merge  $\mathcal{G}_{ffn}^{(\ell)}$  in all layers as  $\mathcal{G}_{ffn}$ :

$$\mathcal{G}_{ffn} = \{W_{:,i}^{(up,\ell)}, W_{:,i}^{(q,\ell)}, W_{i,:}^{(down,\ell)}, \ell = 1, 2, \dots, n\}. \quad (5)$$

3) Per-channel pruning in the transformer stem: When a channel of the transformer stem is pruned, one channel in the token embedding, one input channel in input layer group and one output channel in output layer group for every block, one input channel of the LM head projection is correspondingly pruned at the same time. We donate the stem mini-group as  $\mathcal{G}_{stem}$ :

$$\begin{aligned} \mathcal{G}_{stem} = & \{W_{i,:}^{(k,\ell)}, W_{i,:}^{(q,\ell)}, W_{i,:}^{(v,\ell)}, W_{:,i}^{(o,\ell)}\}, \dots \\ & \cup \{W_{i,:}^{(up,\ell)}, W_{i,:}^{(gate,\ell)}, W_{:,i}^{(down,\ell)}\}, \dots \\ & \cup \{\mathbf{w}_i^{(emb)}, W_{i,:}^{(head)}\}, \quad \ell = 1, 2, \dots, n \end{aligned} \quad (6)$$

216 where  $i$  should be the same in every blocks in Eq. 6;  $i, j$  needn't the same across blocks in Eq. 4,5.  
 217  
 218 Given a transformer with hidden size  $m$ , head number  $h$ , intermediate size  $n$ , and  $l$  layers, the original  
 219 pruning space is  $h^l \times n^l \times m$ . In each pruning step, the mini-groups are dynamically grouped  
 220 by saliency, and we only choose among the 3 types to prune. By coupling the parameters into  
 221 mini-groups, the choice space is reduced to 3 in each step of Eq.3, and the final pruning space is  $3^t$ .  
 222

### 223 3.2 OPTIMIZING MINI-GROUPS BY SALIENCY

224 Based on the mini-groups, Eq.1 becomes a bi-level optimization problem of the mini-groups  $g$  and  
 225 weights  $w$ :  
 226

$$227 \min_{g \in \mathcal{G}} \mathcal{L}_{\text{pretrain}}(g, w^* | \mathcal{M}), \quad \text{s.t.} \quad w^* = \operatorname{argmin}_w \mathcal{L}_{\text{pretrain}}(w, g^* | \mathcal{M}), \quad (7)$$

229 where the outer optimization could be solved by pruning a mini-group in each step as Eq.3, and  
 230 the inner optimization could be directly solved by weight pretraining. The weight pretraining step  
 231 and mini-group optimization (Eq.3) step alternate, and the model size drops continuously during  
 232 pretraining as shown in Fig. 1 (c), until the pre-defined parameter budget is achieved.

233 *Different from vanilla iterative pruning along a predefined trajectory, unified pruning selects its  
 234 pruning trajectory based on saliency.* The pruned model is automatically optimized toward the most  
 235 salient sub-architectures. Thanks to large-scale pretraining data, we find that these saliency-driven  
 236 architectures are competitive with human-designed ones, effectively eliminating the need for manual  
 237 pruning target design and repeated trial-and-error.

238 **Mini-Group Saliency.** In each mini-group selection step, Taylor expansion evaluates the optimal  
 239 mini-group  $g_t^*$  in Eq.3. For an optimized source model, loss of any weight  $w$  can be approximated by  
 240 a second-order Taylor expansion around its optimal value  $w^*$ :

$$242 \mathcal{L}(w) \simeq \mathcal{L}(w^*) + \delta w^\top \nabla \mathcal{L}(w^*) + \frac{1}{2} \delta w^\top \mathbf{H}_{\mathcal{L}}(w^*) \delta w \quad (8)$$

244 where  $\mathcal{L}$ ,  $\nabla \mathcal{L}$ ,  $\mathbf{H}_{\mathcal{L}}$  is the global loss, gradient, hessian matrix; and  $\delta w = w - w^*$ . We substitute  
 245 Eq.8 into Eq.3:  
 246

$$247 \begin{aligned} g_t^* &= \operatorname{argmin}_{g_t \in \mathcal{G}} \mathcal{L}_{\text{pretrain}}(g_t | \mathcal{M}_{t-1}) \\ 248 &= \operatorname{argmin}_{g_t \in \mathcal{G}} g_t^\top \nabla \mathcal{L}(\mathcal{M}_{t-1}) + \frac{1}{2} g_t^\top \mathbf{H}_{\mathcal{L}}(\mathcal{M}_{t-1}) g_t, \end{aligned} \quad (9)$$

252 where we omit the first term  $\mathcal{L}(w^*) = \mathcal{L}(\mathcal{M}_{t-1})$  in Eq.8, because  $\mathcal{L}(\mathcal{M}_{t-1})$  is the same in the step  $t$   
 253 for the 3 mini-groups,  $\mathcal{G} = \{\mathcal{G}_{\text{attn}}, \mathcal{G}_{\text{ffn}}, \mathcal{G}_{\text{stem}}\}$ . And we could calculate mini-group saliency according  
 254 to Eq. 9 (Ma et al., 2023).

255 **Efficient Calculation.** In practice, we only calculate the saliency of the output layer groups for  
 256 efficiency. a neural network is a directed acyclic graph (DAG) (Liu et al., 2018). For each node in the  
 257 graph, pruning all its inputs or all of its outputs is sufficient to prune the entire network. It saves  $2 \sim 3$   
 258 times computation with output layer group only calculation. Details are shown in Fig. 2: 1) *Pruning*  
 259 *Type I*: we only calculate element-wise saliency matrix for the weights of the output projection, and  
 260 then sum each column of the saliency matrix. We select  $\mathcal{G}_{\text{attn}}^{(\ell)}$  based on the lowest row-wise saliency  
 261 in the output projection weights. 2) *Pruning Type II*: we only calculate the element-wise saliency  
 262 matrix for the down projection, and then sum each column.  $\mathcal{G}_{\text{ffn}}^{(\ell)}$  with the lowest row-wise saliency  
 263 are selected. 3) *Pruning Type III*: we already have all the element-wise saliency in the output layer  
 264 group based on Type I and II. To evaluate saliency of the hidden state, we first sum each row of  
 265 saliency matrices, and then, sum the saliency in all of the output layer group.

266 **Hessian Approximations.** Existing post-training methods such as LLM-Pruner (Ma et al., 2023),  
 267 SparseGPT (Frantar & Alistarh, 2023), and Wanda (Sun et al., 2023) have proposed various Hessian  
 268 approximations to approximate hessian matrices. By substituting Eq. 9, our framework can naturally  
 269 extend these post-training pruning methods to the unified pretraining stage. Without loss of generality,  
 we also generalize the second-order weight updating to pretraining in the next subsection.

270 3.3 SECOND-ORDER WEIGHT UPDATING  
271272 Existing second order pruning applies the same Hessian matrix for the pruning weight detection and  
273 the remaining weight updating. However, calculating the global Hessian matrix is impossible in  
274 modern LLMs for its  $\mathcal{O}(n^4)$  complexity. A common approach is to use the squared error at each layer  
275 as a proxy for the global loss:  $\mathbf{H}_{\mathcal{L}} \simeq \mathbf{X} \mathbf{X}^T$ , such as in SparseGPT (Frantar & Alistarh, 2023), OBC  
276 (Frantar & Alistarh, 2022). Although achieving the  $\mathcal{O}(d_{row} \times d_{col}^2)$  complexity, Hessian matrices  
277 can not describe the global loss.278 This work addresses this problem by decoupling the Hessian matrix in saliency detection and weight  
279 updating. To capture global saliency, we approximate with global diagonal Hessian matrices as  
280 LLM-Pruner for saliency detection; to reduce computational complexity, we apply the layerwise  
281 proxy Hessian,  $\mathbf{H}_{\mathcal{L}} \simeq \mathbf{X} \mathbf{X}^T$ , for weight updating. In each step, we prune a mini-group including only  
282 one column of weights in a layer, and the remaining weights are updated by  $\delta w_p = -\frac{w_p}{[\mathbf{H}^{-1}]_{pp}} \cdot \mathbf{H}_{:,p}^{-1}$ .  
283 To efficiently compute the  $p$ -th column of the inverse Hessian matrix  $\mathbf{H}_{:,p}^{-1}$ , it suffices to solve the  
284 linear equation  $\mathbf{H} \mathbf{H}_{:,p}^{-1} = \mathbf{e}_p$  in a weight updating step.  
285286 4 EXPERIMENTS  
287288 **Models.** To compare with the most general post-training pruning, EfficientLLM-A basically approxi-  
289 mates Eq.9 as LLM-Pruner. EfficientLLM-B additionally applies the second-order weight updating  
290 based on EfficientLLM-A. 1) In empirical studies, we evaluate EfficientLLM with SmolLM-1.7B  
291 (Allal et al., 2024), Llama2-7B (Touvron et al., 2023b), and Qwen2.5-7B (Yang et al., 2024b) as the  
292 source models. 2) In main results, we prolong and pretrain EfficientLLM-134M from the source  
293 model SmolLM-360M; EfficientLLM-457M and 1.1B from SmolLM-1.7B. 3) In comparisons with  
294 LLM pruning, we keep the Llama-7B (Touvron et al., 2023a) source model.  
295296 **Data Composition.** EfficientLLM maintains a data distribution similar to the source model: 1)  
297 in main results, our pretraining data composition is similar to SmolLM, including 220B tokens  
298 from FineWeb-Edu (Lozhkov et al., 2024), 28B tokens from Cosmopedia v2 (Ben Allal et al.,  
299 2024a), 4B tokens from Python-Edu (Ben Allal et al., 2024b), and 27.5B tokens randomly sampled  
300 from OpenWebMath (Paster et al., 2023). 2) In comparisons with LLM pruning, we sample from  
301 RedPajama-1T (Weber et al., 2024) as pretraining data with the Llama family as the source model.302 **Training.** In main results, we use the 2 stage pretraining as ShearedLlama (Xia et al., 2023) but  
303 explore in large scale: the large scale unified pruning followed by the continued pretraining. For  
304 EfficientLLM-134M, 460M, and 1.1B, we pretrain 50.3B, 72.1B, and 36.7B tokens for unified  
305 pruning followed by 500B, 500B, and 320B tokens continued pretraining. Note that the large-scale  
306 continued pretraining is not necessary, and 50B tokens also achieve competitive performance. Note  
307 also that the number of tokens used for unified pruning is determined by the number of iterations  
308 required to reach the target parameter count. All the training details are shown in Appendix B.1.309 **Evaluations.** For pretrained base models, we follow Llama, MobileLLM, and ShearedLlama to  
310 evaluate Common Sense Reasoning tasks: ARC (Clark et al., 2018), BoolQ (Clark et al., 2019),  
311 HellaSwag (Zellers et al., 2019), OBQA (Mihaylov et al., 2018), PIQA (Bisk et al., 2020), and  
312 WinoGrande (Sakaguchi et al., 2021). The MMLU (Hendrycks et al., 2020) for Word Knowledge  
313 evaluation is also applied. For instruct finetuned model, we use the standard Alpaca-Eval (Li et al.,  
314 2023) with GPT-4o as the judge model.315 4.1 EMPIRICAL STUDIES  
316

317 As shown in Table 1, 2, 3, we train around 450M target models from the source model SmolLM-1.7B.

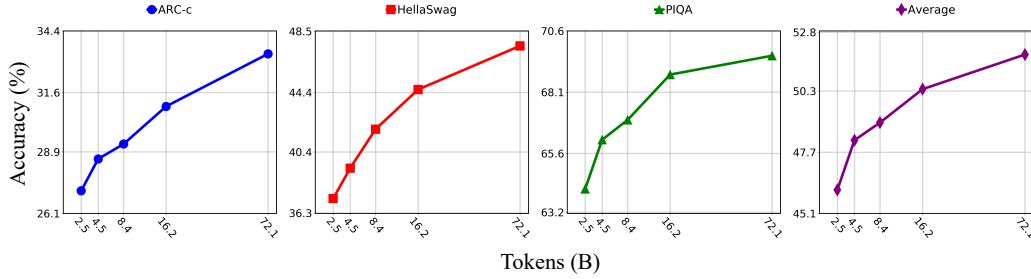
318 **Training Schemes.** We first compare the efficiency of different training schemes under the same 5B  
319 token budget: 1) Direct Pretraining: three architectures are pretrained from scratch using 5B tokens:  
320 (i) Direct-hidden: Prunes the hidden size of the source architecture. (ii) Direct-source: Uniformly  
321 scales down the source model. (iii) Searched architecture: Uses the architecture searched by Unified  
322 Pruning. 2) ShearedLlama: Requires manually specified pruning targets. We consider two variants:  
323 pruning hidden size or uniformly scaling the source model. 3) Unified Few-shot Pruning: Applies

324 Table 1: Comparison of different training schemes under **the same token budget**. 1) Direct pretrain-  
 325 ing: "hidden" or "source" indicates target architectures from the source model. 2) Comparison with  
 326 ShearedLlama in >70% pruning ratio. 3) Comparison with LLM-Pruner with continued pretraining in  
 327 smaller pruning ratios. We prune both LLaMA2-7B and Qwen2.5-7B for 4000 steps to 3.3B and 5.2B.

328 Model	329 Source	330 ARC-c	331 ARC-e	332 BoolQ	333 HellaSwag	334 OBQA	335 PIQA	336 WinoGrande	Avg.
328 Direct-hidden	329 -	330 26.88	331 55.85	332 52.39	333 37.10	334 30.20	335 66.65	336 50.51	45.65
328 Direct-source	329 -	330 28.67	331 59.68	332 56.30	333 38.41	334 32.00	335 65.67	336 49.96	47.24
328 Searched Arch. (Ours)	329 -	330 29.10	331 59.30	332 61.38	333 37.74	334 32.80	335 66.76	336 51.07	48.30
328 ShearedLlama-hidden	329 SmoLLM-1.7B	330 28.41	331 57.41	332 60.98	333 39.79	334 30.80	335 66.81	336 54.06	48.32
328 ShearedLlama-source	329 SmoLLM-1.7B	330 30.89	331 62.08	332 61.07	333 44.29	334 32.60	335 68.39	336 52.25	50.22
328 Unified FewShot Prun.	329 SmoLLM-1.7B	330 30.63	331 62.67	332 61.22	333 44.31	334 34.00	335 68.66	336 53.43	50.25
328 <b>EfficientLLM-A</b>	329 SmoLLM-1.7B	330 30.46	331 <b>64.06</b>	332 <b>61.99</b>	333 45.98	334 34.00	335 <b>69.91</b>	336 53.91	51.47
328 <b>EfficientLLM-B</b>	329 SmoLLM-1.7B	330 <b>30.97</b>	331 63.22	332 60.86	333 <b>46.51</b>	334 <b>35.00</b>	335 69.64	336 <b>55.09</b>	<b>51.61</b>
328 LLM-Pruner	329 LLaMA2-7B	330 27.30	331 43.52	332 61.10	333 38.15	334 29.40	335 63.11	336 51.14	44.82
328 <b>EfficientLLM-A</b>	329 LLaMA2-7B	330 <b>32.76</b>	331 <b>57.53</b>	332 <b>65.96</b>	333 <b>53.07</b>	334 <b>33.80</b>	335 <b>69.42</b>	336 <b>58.09</b>	<b>52.95</b>
328 LLM-Pruner	329 Qwen2.5-7B	330 38.40	331 66.67	332 70.58	333 57.97	334 38.40	335 72.52	336 60.62	57.88
328 <b>EfficientLLM-A</b>	329 Qwen2.5-7B	330 <b>40.10</b>	331 <b>70.50</b>	332 <b>76.79</b>	333 <b>61.26</b>	334 <b>40.80</b>	335 <b>73.34</b>	336 <b>61.72</b>	<b>60.64</b>

337 Table 2: Generalization to various pruning metrics. LLM-Pruner (Ma et al., 2023), OBC (Frantar  
 338 & Alistarh, 2022), Diag-Hessian (Sun et al., 2023; LeCun et al., 1989) metrics are embedded in the  
 339 unified pruning. All results are without continued pretraining.

341 Model	342 ARC-c	343 ARC-e	344 BoolQ	345 HellaSwag	346 OBQA	347 PIQA	348 WinoGrande	349 Avg.
341 LLM-Pruner	342 22.18	343 26.64	344 49.63	345 25.62	346 27.80	347 51.20	348 50.59	349 36.24
341 +Unified Pruning	342 29.18	343 57.79	344 59.57	345 41.93	346 34.40	347 66.97	348 52.88	349 <b>48.96</b>
341 OBC (SparseGPT)	342 25.51	343 25.88	344 37.86	345 26.81	346 29.20	347 51.41	348 50.51	349 35.31
341 +Unified Pruning	342 29.44	343 60.02	344 62.02	345 42.27	346 33.40	347 67.41	348 53.35	349 <b>49.70</b>
341 Diag-Hess (Wanda, OBD)	342 25.85	343 25.88	344 50.80	345 26.06	346 30.40	347 51.69	348 48.22	349 36.99
341 +Unified Pruning	342 29.95	343 60.14	344 60.83	345 41.68	346 32.80	347 66.38	348 52.88	349 <b>49.24</b>



355 Figure 3: Scalability of unified pruning-aware pretraining without continued pretraining.

356 Table 3: Ablation studies on the unified pruning-aware pretraining. "Direct Training" keeps the same  
 357 architecture ratio as the source model. "Pruned Arch." indicates the auto-designed architecture.

360 Model	361 ARC-c	362 ARC-e	363 BoolQ	364 HellaSwag	365 OBQA	366 PIQA	367 WinoGrande	368 Avg.
361 Direct Training	362 28.67	363 59.68	364 56.30	365 38.41	366 32.00	367 65.67	368 49.96	369 47.24
361 +Searched Arch.	362 29.10	363 59.30	364 61.38	365 37.74	366 32.80	367 66.76	368 51.07	369 48.30
361 +Unified FewShot Pruning	362 30.63	363 62.67	364 61.22	365 44.31	366 34.00	367 68.66	368 53.43	369 50.25
361 +Prolong Pruning	362 34.13	363 66.16	364 60.49	365 49.87	366 <b>35.80</b>	367 70.67	368 54.30	369 53.06
361 +Prolong Continued Pretrain.	362 <b>35.92</b>	363 <b>70.50</b>	364 <b>59.85</b>	365 <b>53.16</b>	366 35.00	367 <b>72.69</b>	368 <b>56.27</b>	369 <b>54.77</b>

370 mini-group optimization on 128 samples using LLM-Pruner's metric, followed by training on 5B  
 371 tokens. 4) Unified Pruning-aware Pretraining: Follows the ShearedLlama pipeline, pruning with 1B  
 372 tokens, then continuing training on the remaining 4B tokens.

373 We evaluate the necessity of unified architecture auto-design, pruning, and pretraining in Table 1: 1)  
 374 **Architecture matters:** For directly pretrained edge models, the choice of architecture significantly  
 375 impacts performance. The searched Arch. outperforms Direct-hidden by 2.7%. 2) **Pruning boosts**  
 376 **edge models:** With the same architecture, Unified Pruning-aware Pretraining surpasses Search Arch.  
 377 by 3.17%. 3) **Scaling up pruning can benefit more than finetuning:** Compared to Unified Few-  
 378 shot Pruning, Pruning-aware pretraining allocates more tokens to the pruning stage and improves  
 379 accuracy by 1.22%. Unlike ShearedLlama, Unified Pruning requires no manual architecture design.  
 380 For example, ShearedLlama-hidden adopts a suboptimal target, resulting in 3.15% accuracy drop.

381 **Pruning Metrics.** We embed well-studied post-training pruning metrics in our Unified Pruning-aware  
 382 Pretraining, enhancing performance of existing methods. By replacing Eq. 9, we apply LLM-Pruner

378 Table 4: Zero-shot performance on World Knowledge and Common Sense Reasoning tasks. “Avg.”  
379 calculate among the 7 Common Sense Reasoning tasks. #Tokens count continued pretraining for  
380 EfficientLLM. All the results are evaluated on the same evaluation (Appendix B.2).

Model	#Tokens	#Params	MMLU	ARC-c	ARC-e	BoolQ	HellaSwag	OBQA	PIQA	Winogrande	Avg.
OPT-125M	180B	125M	26.02	22.87	43.31	55.44	31.37	27.80	62.62	49.80	41.89
GPT-neo-125M	300B	125M	26.89	23.29	43.22	61.77	30.49	26.00	62.62	51.93	42.76
Pythia-160M	300B	162M	26.43	22.27	37.84	43.33	29.97	26.40	58.87	49.96	38.38
Mamba-130M	1.2T	130M	27.65	24.49	47.56	54.68	35.11	29.00	64.69	53.35	44.13
MobileLLM-125M	1T	125M	27.58	24.32	46.38	60.34	38.15	28.40	65.13	52.41	45.02
SmolLM-135M	600B	135M	30.05	29.35	61.32	59.85	42.67	<b>34.40</b>	68.55	52.96	49.87
EfficientLLM-A	500B	134M	<b>30.54</b>	<b>30.97</b>	<b>62.88</b>	<b>60.40</b>	<b>43.81</b>	33.60	<b>68.82</b>	<b>53.28</b>	<b>50.54</b>
OPT-350M	180B	331M	26.96	23.98	44.02	57.80	36.63	27.80	64.91	52.96	44.01
BLOOM-560M	350B	559M	27.32	24.40	46.04	44.46	36.54	28.80	62.57	53.20	42.29
Pythia-410M	300B	405M	29.10	24.15	51.39	59.20	40.20	29.40	66.70	53.83	46.41
MobileLLM-350M	1T	345M	30.21	27.39	56.40	61.96	49.51	31.00	68.88	57.14	50.33
SmolLM-360M	600B	362M	33.89	36.26	70.16	55.23	53.51	37.60	71.38	57.22	54.48
Qwen2-0.5B	15T	494M	31.85	28.50	55.05	61.25	49.16	32.80	69.75	57.22	50.53
Qwen2.5-0.5B	17T	494M	33.37	32.17	64.44	61.99	52.09	35.20	70.29	56.20	53.20
EfficientLLM-A	50B	457M	33.09	35.92	70.50	59.85	53.16	35.00	72.69	56.27	54.77
EfficientLLM-A	500B	457M	<b>34.54</b>	<b>38.40</b>	<b>72.10</b>	<b>62.42</b>	<b>56.84</b>	<b>40.40</b>	<b>73.83</b>	<b>57.46</b>	<b>57.35</b>
OPT-1.3B	180B	1.3B	29.57	30.03	57.49	56.54	53.66	32.80	72.31	59.04	51.70
GPT-neo-1.3B	380B	1.3B	30.00	25.94	56.31	61.90	48.99	33.40	71.00	54.62	50.31
BLOOM-1.1B	350B	1.1B	29.16	25.77	51.73	59.51	43.11	29.60	67.30	54.62	47.38
Pythia-1B	300B	1.0B	30.14	26.96	56.86	60.04	47.15	31.20	70.29	52.88	49.34
TinyLlama-1.1B	3T	1.1B	32.30	30.29	60.40	56.85	59.13	35.80	73.07	59.04	53.51
ShearedLlama-1.3B	50B	1.3B	31.51	29.44	61.07	61.83	59.33	34.40	73.94	58.01	54.00
OLMo-1B	2T	1.2B	32.03	30.72	63.55	61.38	62.86	36.40	75.35	59.35	55.66
Llama3.2-1B	—	1.2B	36.31	31.48	65.28	63.88	63.69	37.40	74.59	60.54	56.69
EfficientLLM-A	50B	1.1B	36.71	40.36	73.61	62.39	60.24	40.20	75.19	61.25	59.03
EfficientLLM-A	320B	1.1B	<b>37.71</b>	<b>42.24</b>	<b>73.48</b>	<b>67.09</b>	<b>64.09</b>	<b>41.80</b>	<b>75.41</b>	<b>61.17</b>	<b>60.75</b>

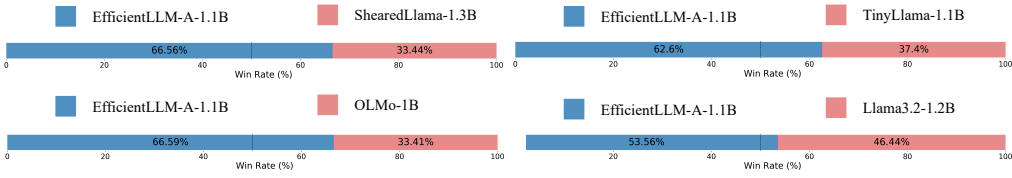


Figure 4: Win rate of EfficientLLM in the instruction tuning task.

and diagonal Hessian-based metrics into Unified Pruning. We further extend this by adding second-order weight updates (Section 3.3) to support OBC-based methods. Reaching the pruning target takes about 4,000 steps with a batch size of 1M tokens. As shown in Table 2, LLM-Pruner, OBC, and diagonal Hessian metrics improve accuracy by 12.72%, 14.39%, and 12.25%, respectively. According to Appendix B.5, EfficientLLM-B performs better in small scale pretraining, and similar in large scale. For generality, we apply the LLM-pruner metric in main results.

**Ablation Studies.** To evaluate each part of the unified pruning, we decouple into 3 basic designs to improve edge language model pretraining: the auto-designed architecture, pruning, and scalable pruning stage. As shown in Fig. 3, we scale up unified pruning according to Appendix B.3. As shown in Table 3, the pruned architecture, unified pruning, and scaling up pruning with 78B tokens continuously improve 5.82% accuracy. We further scale up finetuning (or continued pretraining) to 50B tokens, as in ShearedLlama, and achieve 7.53% accuracy overall.

**Architecture Robustness.** In Appendix A.1, architectures are stably optimized according to dynamic saliency. In Appendix A.2, we evaluate different pruning trajectories to reach the searched architecture. Once we find the optimal architecture, a different trajectory can achieve the same or better results, which we refer to the generalized Lottery Ticket Hypothesis (Frankle & Carbin, 2018).

## 4.2 MAIN RESULTS

**Edge Language Modeling.** For fair comparison, we collect main streams of edge language models in  $100M \sim 1B$  sizes, evaluate in the same conditions (Appendix B.2), and make a benchmark in Table 4. 1) Early edge models including OPT (Zhang et al., 2023b), GPT-neo (Black et al., 2022), Pythia (Biderman et al., 2023), and BLOOM (Le Scao et al., 2023) are direct pretrained in limited tokens and sub-optimal architectures, which largely hinder the performance. By leveraging unified pruning, EfficientLLM achieves both architecture and data efficiency. For instance, EfficientLLM-134M exceeds Pythia-410M by 4.13% average accuracy; EfficientLLM-1.1B with 50B tokens exceeds OLMo-1B, TinyLlama, Llama3.2-1B in accuracy. 2) Compared with the SoTA edge model MobileLLM (Liu et al., 2024b), EfficientLLM-134M exceeds MobileLLM-125M by 5.52% with the large scale model compression. 3) Recent SoTA industrial models scaling up pretraining tokens

432 Table 5: Comparisons of LLM pruning in Llama-7B. We scale up pruning-aware pretraining to 5B  
 433 tokens for EfficientLLM. #Tuning donates whether to finetune after pruning. Most works report  
 434 finetuned results.

#Ratio	Model	#Tuning	ARC-c	ARC-e	BoolQ	HellaSwag	OBQA	PIQA	WinoGrande	Avg.
50%	MaP	✓	30.63	49.32	39.69	42.49	31.40	66.81	50.67	44.43
	MvP	✓	26.79	44.07	59.94	40.98	31.80	63.06	55.64	46.04
	WANDA	✓	34.20	42.68	50.90	38.12	38.78	57.38	55.98	45.43
	LLM-Pruner	✓	28.24	46.46	61.47	47.56	35.20	68.82	55.09	48.98
	LoRAPrune	✓	31.62	45.13	61.88	47.86	34.98	71.53	55.01	49.72
	LoRAShear	✓	32.26	47.68	62.12	48.01	34.61	71.80	56.29	50.40
	Compresso	✓	27.82	48.82	60.09	39.31	33.40	66.70	51.93	46.87
	NutePrune	✗	31.74	46.59	62.20	53.87	35.80	69.91	57.77	51.13
	NutePrune	✓	32.17	51.68	62.26	55.88	34.40	71.00	57.54	52.13
	EfficientLLM-A	✗	30.80	52.15	62.29	54.70	35.20	71.33	56.75	51.89
	EfficientLLM-A	✓	<b>34.04</b>	<b>64.81</b>	<b>64.83</b>	<b>60.12</b>	<b>34.60</b>	<b>73.88</b>	<b>61.48</b>	<b>56.25</b>
70%	LLM-Pruner	✓	24.83	39.56	47.28	31.66	28.80	60.83	50.75	40.53
	NutePrune	✓	26.19	42.17	62.08	39.43	30.20	62.30	51.46	44.83
	EfficientLLM-A	✗	27.73	54.50	47.89	47.77	31.00	68.17	55.17	47.46
	EfficientLLM-A	✓	<b>29.95</b>	<b>58.59</b>	<b>58.13</b>	<b>52.02</b>	<b>34.60</b>	<b>70.08</b>	<b>55.96</b>	<b>51.33</b>

446 like Qwen (Yang et al., 2024a;b) and Llama3.2-1B, EfficientLLM-457M and 1.1B outperforms  
 447 Qwen2.5-0.5B by 4.15% and Llama3.2-1B by 4.06% respectively with limited pretraining data. As  
 448 shown in Appendix C.1, EfficientLLM-457M achieves higher accuracy while requiring **62**× and **16**×  
 449 fewer GPU hours than Qwen2.5-0.5B when using 50B and 500B continued pretraining tokens.  
 450

451 **Instruction Tuning.** We finetune EfficientLLM-1.1B and other top-quality open-source base models  
 452 includes OLMo-1B, ShearedLlama-1.3B, TinyLlama-1.1B and Llama3.2-1B in the same condition.  
 453 We finetune on the Alpaca dataset (Taori et al., 2023) with 52K instructions for 3 epochs. As shown  
 454 in Fig. 4, EfficientLLM-1.1B significantly outperforms SoTA baselines, indicating the generalization  
 455 ability in the supervised finetuning (SFT). More case studies are shown in Appendix D.

456 **Inference Speed & Quantization.** Most edge devices are non-GPU environments. We deploy edge  
 457 models using 1, 2, 4, and 8 Intel Xeon @ 2.90GHz CPUs respectively. As shown in Appendix  
 458 C.2, when using 2 CPUs, EfficientLLM-457M speeds up  $\times 8.7$  and  $\times 3.2$  than MobileLLM-350M  
 459 and Qwen2.5-0.5B respectively; EfficientLLM-1B speeds up  $\times 7.3$  and  $\times 1.2$  than OLMo-1B and  
 460 Llama3.2-1B. In Appendix C.3, we further quantize EfficientLLM with 8 bit weights and 8 bit  
 461 activations (8W8A) using the general OmniQuant (Shao et al., 2023). After 8W8A quantization,  
 462 EfficientLLM-457M even improves 0.09% and EfficientLLM-1B only drops 0.27% average accuracy.  
 463

### 4.3 COMPARISONS WITH LLM PRUNING

465 We mainly focus on large pruning ratio because it is more practical to achieve highly efficiency  
 466 based on heavy source LLMs. In Table 5, we scale up pruning-aware pretraining to only 5B  
 467 tokens. We report both results with or without finetuning after pruning. Because previous works  
 468 finetune in different settings, we finetune additional 1B tokens if with it. Notice that, even without  
 469 finetuning, EfficientLLM exceeds all the according baselines. It is shown that existing LLM pruning  
 470 is impractical in large pruning ratio. By simply scaling up LLM-Pruner metric in pruning-aware  
 471 pretraining, EfficientLLM-A significantly exceeds SoTA NutePrune 6.5% in 70% ratio without bells  
 472 and whistles, while NutePrune integrates distillation and additional learnable masks. In 50% ratio,  
 473 EfficientLLM exceeds LoRAPrune by 2.18% and 6.54% when with and without tuning. Experiments  
 474 reveal that only scaling up the pruning stage to 5B tokens can achieve much higher performance than  
 475 previous results, highlighting the importance of scalable pruning methods.

## 476 5 CONCLUSION

477 This work primarily advances the edge language model pretraining to exceed the traditional LLM  
 478 scaling law. Distinguished from almost LLM compression in post-training, this work scales up  
 479 existing pruning metric in the pretraining stage, promoting LLM compression to the era of pretraining.  
 480 Technically, minimal parameter groups are defined and optimized by saliency to address scalable  
 481 target-agnostic pruning. The results reveal that even if vanilla LLM-Pruner can surpass SoTA pruning  
 482 methods by scaling up and outperform direct pretraining edge models.

483 **Limitations.** Future work will explore the reasoning and long-context capabilities of edge language  
 484 models. Since reasoning is more related to CoT data and base models, we exclude it in this work.

486  
487  
**ETHICS STATEMENT**488  
489  
490  
491  
492  
493  
494  
495  
496  
497  
498  
499  
500  
501  
502  
503  
504  
505  
506  
507  
508  
509  
510  
511  
512  
513  
514  
515  
516  
517  
518  
519  
520  
521  
522  
523  
524  
525  
526  
527  
528  
529  
530  
531  
532  
533  
534  
535  
536  
537  
538  
539  
All authors have read and agree to adhere to the ICLR Code of Ethics. This paper presents work  
whose goal is to advance the field of Machine Learning. At present, we do not identify any specific  
ethical concerns that require special attention beyond standard considerations of fairness, privacy,  
security, and research integrity.500  
501  
502  
503  
504  
505  
506  
507  
508  
509  
510  
511  
512  
513  
514  
515  
516  
517  
518  
519  
520  
521  
522  
523  
524  
525  
526  
527  
528  
529  
530  
531  
532  
533  
534  
535  
536  
537  
538  
539  
**REPRODUCIBILITY STATEMENT**500  
501  
502  
503  
504  
505  
506  
507  
508  
509  
510  
511  
512  
513  
514  
515  
516  
517  
518  
519  
520  
521  
522  
523  
524  
525  
526  
527  
528  
529  
530  
531  
532  
533  
534  
535  
536  
537  
538  
539  
We release the code in supplemental materials. All of the training data and evaluation methods are  
publicly available with clear source.500  
501  
502  
503  
504  
505  
506  
507  
508  
509  
510  
511  
512  
513  
514  
515  
516  
517  
518  
519  
520  
521  
522  
523  
524  
525  
526  
527  
528  
529  
530  
531  
532  
533  
534  
535  
536  
537  
538  
539  
**REFERENCES**500  
501  
502  
503  
504  
505  
506  
507  
508  
509  
510  
511  
512  
513  
514  
515  
516  
517  
518  
519  
520  
521  
522  
523  
524  
525  
526  
527  
528  
529  
530  
531  
532  
533  
534  
535  
536  
537  
538  
539  
Josh Achiam, Steven Adler, Sandhini Agarwal, Lama Ahmad, Ilge Akkaya, Florencia Leoni Aleman,  
Diogo Almeida, Janko Altenschmidt, Sam Altman, Shyamal Anadkat, et al. Gpt-4 technical report.  
*arXiv preprint arXiv:2303.08774*, 2023.500  
501  
502  
503  
504  
505  
506  
507  
508  
509  
510  
511  
512  
513  
514  
515  
516  
517  
518  
519  
520  
521  
522  
523  
524  
525  
526  
527  
528  
529  
530  
531  
532  
533  
534  
535  
536  
537  
538  
539  
Joshua Ainslie, James Lee-Thorp, Michiel de Jong, Yury Zemlyanskiy, Federico Lebrón, and Sumit  
Sanghai. Gqa: Training generalized multi-query transformer models from multi-head checkpoints.  
*arXiv preprint arXiv:2305.13245*, 2023.500  
501  
502  
503  
504  
505  
506  
507  
508  
509  
510  
511  
512  
513  
514  
515  
516  
517  
518  
519  
520  
521  
522  
523  
524  
525  
526  
527  
528  
529  
530  
531  
532  
533  
534  
535  
536  
537  
538  
539  
Loubna Ben Allal, Anton Lozhkov, Elie Bakouch, Leandro von Werra, and Thomas Wolf. Smollm -  
blazingly fast and remarkably powerful, 2024.500  
501  
502  
503  
504  
505  
506  
507  
508  
509  
510  
511  
512  
513  
514  
515  
516  
517  
518  
519  
520  
521  
522  
523  
524  
525  
526  
527  
528  
529  
530  
531  
532  
533  
534  
535  
536  
537  
538  
539  
Saleh Ashkboos, Maximilian L Croci, Marcelo Gennari do Nascimento, Torsten Hoefer, and James  
Hensman. Slicecpt: Compress large language models by deleting rows and columns. *arXiv*  
*preprint arXiv:2401.15024*, 2024.500  
501  
502  
503  
504  
505  
506  
507  
508  
509  
510  
511  
512  
513  
514  
515  
516  
517  
518  
519  
520  
521  
522  
523  
524  
525  
526  
527  
528  
529  
530  
531  
532  
533  
534  
535  
536  
537  
538  
539  
Loubna Ben Allal, Anton Lozhkov, Guilherme Penedo, Thomas Wolf, and Leandro von Werra.  
Cosmopedia, 2024a. URL <https://huggingface.co/datasets/HuggingFaceTB/cosmopedia>.500  
501  
502  
503  
504  
505  
506  
507  
508  
509  
510  
511  
512  
513  
514  
515  
516  
517  
518  
519  
520  
521  
522  
523  
524  
525  
526  
527  
528  
529  
530  
531  
532  
533  
534  
535  
536  
537  
538  
539  
Loubna Ben Allal, Anton Lozhkov, Guilherme Penedo, Thomas Wolf, and Leandro von Werra.  
Smollm-corpus, 2024b. URL <https://huggingface.co/datasets/HuggingFaceTB/smollm-corpus>.500  
501  
502  
503  
504  
505  
506  
507  
508  
509  
510  
511  
512  
513  
514  
515  
516  
517  
518  
519  
520  
521  
522  
523  
524  
525  
526  
527  
528  
529  
530  
531  
532  
533  
534  
535  
536  
537  
538  
539  
Adithya Bhaskar, Alexander Wettig, Dan Friedman, and Danqi Chen. Finding transformer circuits  
with edge pruning. *arXiv preprint arXiv:2406.16778*, 2024.500  
501  
502  
503  
504  
505  
506  
507  
508  
509  
510  
511  
512  
513  
514  
515  
516  
517  
518  
519  
520  
521  
522  
523  
524  
525  
526  
527  
528  
529  
530  
531  
532  
533  
534  
535  
536  
537  
538  
539  
Stella Biderman, Hailey Schoelkopf, Quentin Gregory Anthony, Herbie Bradley, Kyle O'Brien, Eric  
Hallahan, Mohammad Aflah Khan, Shivanshu Purohit, USVSN Sai Prashanth, Edward Raff, et al.  
Pythia: A suite for analyzing large language models across training and scaling. In *International  
Conference on Machine Learning*, pp. 2397–2430. PMLR, 2023.500  
501  
502  
503  
504  
505  
506  
507  
508  
509  
510  
511  
512  
513  
514  
515  
516  
517  
518  
519  
520  
521  
522  
523  
524  
525  
526  
527  
528  
529  
530  
531  
532  
533  
534  
535  
536  
537  
538  
539  
Yonatan Bisk, Rowan Zellers, Jianfeng Gao, Yejin Choi, et al. Piqa: Reasoning about physical  
commonsense in natural language. In *Proceedings of the AAAI conference on artificial intelligence*,  
volume 34, pp. 7432–7439, 2020.500  
501  
502  
503  
504  
505  
506  
507  
508  
509  
510  
511  
512  
513  
514  
515  
516  
517  
518  
519  
520  
521  
522  
523  
524  
525  
526  
527  
528  
529  
530  
531  
532  
533  
534  
535  
536  
537  
538  
539  
Sid Black, Stella Biderman, Eric Hallahan, Quentin Anthony, Leo Gao, Laurence Golding, Horace He,  
Connor Leahy, Kyle McDonell, Jason Phang, et al. Gpt-neox-20b: An open-source autoregressive  
language model. *arXiv preprint arXiv:2204.06745*, 2022.500  
501  
502  
503  
504  
505  
506  
507  
508  
509  
510  
511  
512  
513  
514  
515  
516  
517  
518  
519  
520  
521  
522  
523  
524  
525  
526  
527  
528  
529  
530  
531  
532  
533  
534  
535  
536  
537  
538  
539  
Tom Brown, Benjamin Mann, Nick Ryder, Melanie Subbiah, Jared D Kaplan, Prafulla Dhariwal,  
Arvind Neelakantan, Pranav Shyam, Girish Sastry, Amanda Askell, et al. Language models are  
few-shot learners. *Advances in neural information processing systems*, 33:1877–1901, 2020.500  
501  
502  
503  
504  
505  
506  
507  
508  
509  
510  
511  
512  
513  
514  
515  
516  
517  
518  
519  
520  
521  
522  
523  
524  
525  
526  
527  
528  
529  
530  
531  
532  
533  
534  
535  
536  
537  
538  
539  
Christopher Clark, Kenton Lee, Ming-Wei Chang, Tom Kwiatkowski, Michael Collins, and Kristina  
Toutanova. Boolq: Exploring the surprising difficulty of natural yes/no questions. *arXiv preprint  
arXiv:1905.10044*, 2019.

540 Peter Clark, Isaac Cowhey, Oren Etzioni, Tushar Khot, Ashish Sabharwal, Carissa Schoenick, and  
 541 Oyvind Tafjord. Think you have solved question answering? try arc, the ai2 reasoning challenge.  
 542 *arXiv preprint arXiv:1803.05457*, 2018.

543

544 Peijie Dong, Lujun Li, Zhenheng Tang, Xiang Liu, Xinglin Pan, Qiang Wang, and Xiaowen Chu.  
 545 Pruner-zero: Evolving symbolic pruning metric from scratch for large language models. *arXiv*  
 546 *preprint arXiv:2406.02924*, 2024.

547 Abhimanyu Dubey, Abhinav Jauhri, Abhinav Pandey, Abhishek Kadian, Ahmad Al-Dahle, Aiesha  
 548 Letman, Akhil Mathur, Alan Schelten, Amy Yang, Angela Fan, et al. The llama 3 herd of models.  
 549 *arXiv preprint arXiv:2407.21783*, 2024.

550

551 Clémentine Fourrier, Nathan Habib, Thomas Wolf, and Lewis Tunstall. Lighteval: A lightweight  
 552 framework for llm evaluation, 2023. URL <https://github.com/huggingface/lighteval>.

553

554 Jonathan Frankle and Michael Carbin. The lottery ticket hypothesis: Finding sparse, trainable neural  
 555 networks. *arXiv preprint arXiv:1803.03635*, 2018.

556

557 Elias Frantar and Dan Alistarh. Optimal brain compression: A framework for accurate post-training  
 558 quantization and pruning. *Advances in Neural Information Processing Systems*, 35:4475–4488,  
 559 2022.

560 Elias Frantar and Dan Alistarh. Sparsegpt: Massive language models can be accurately pruned in  
 561 one-shot. In *International Conference on Machine Learning*, pp. 10323–10337. PMLR, 2023.

562

563 Leo Gao, Jonathan Tow, Baber Abbasi, Stella Biderman, Sid Black, Anthony DiPofi, Charles Foster,  
 564 Laurence Golding, Jeffrey Hsu, Alain Le Noac'h, Haonan Li, Kyle McDonell, Niklas Muennighoff,  
 565 Chris Ociepa, Jason Phang, Laria Reynolds, Hailey Schoelkopf, Aviya Skowron, Lintang Sutawika,  
 566 Eric Tang, Anish Thite, Ben Wang, Kevin Wang, and Andy Zou. A framework for few-shot  
 567 language model evaluation, 07 2024. URL <https://zenodo.org/records/12608602>.

568

569 Dirk Groeneveld, Iz Beltagy, Pete Walsh, Akshita Bhagia, Rodney Kinney, Oyvind Tafjord,  
 570 Ananya Harsh Jha, Hamish Ivison, Ian Magnusson, Yizhong Wang, et al. Olmo: Accelerating  
 571 the science of language models. *arXiv preprint arXiv:2402.00838*, 2024.

572

573 Yuxian Gu, Li Dong, Furu Wei, and Minlie Huang. Minillm: Knowledge distillation of large language  
 574 models. In *The Twelfth International Conference on Learning Representations*, 2024.

575

576 Daya Guo, Dejian Yang, Haowei Zhang, Junxiao Song, Ruoyu Zhang, Runxin Xu, Qihao Zhu,  
 577 Shirong Ma, Peiyi Wang, Xiao Bi, et al. Deepseek-r1: Incentivizing reasoning capability in llms  
 578 via reinforcement learning. *arXiv preprint arXiv:2501.12948*, 2025.

579

580 Song Han, Huizi Mao, and William J Dally. Deep compression: Compressing deep neural networks  
 581 with pruning, trained quantization and huffman coding. *arXiv preprint arXiv:1510.00149*, 2015.

582

583 Babak Hassibi, David G Stork, and Gregory J Wolff. Optimal brain surgeon and general network  
 584 pruning. In *IEEE international conference on neural networks*, pp. 293–299. IEEE, 1993.

585

586 Dan Hendrycks, Collin Burns, Steven Basart, Andy Zou, Mantas Mazeika, Dawn Song, and  
 587 Jacob Steinhardt. Measuring massive multitask language understanding. *arXiv preprint*  
 588 *arXiv:2009.03300*, 2020.

589

590 Jared Kaplan, Sam McCandlish, Tom Henighan, Tom B Brown, Benjamin Chess, Rewon Child, Scott  
 591 Gray, Alec Radford, Jeffrey Wu, and Dario Amodei. Scaling laws for neural language models.  
 592 *arXiv preprint arXiv:2001.08361*, 2020.

593

594 Jongwoo Ko, Sungnyun Kim, Tianyi Chen, and Se-Young Yun. Distillm: Towards streamlined  
 595 distillation for large language models. *arXiv preprint arXiv:2402.03898*, 2024.

596

597 Teven Le Scao, Angela Fan, Christopher Akiki, Ellie Pavlick, Suzana Ilić, Daniel Hesslow, Roman  
 598 Castagné, Alexandra Sasha Luccioni, François Yvon, Matthias Gallé, et al. Bloom: A 176b-  
 599 parameter open-access multilingual language model. 2023.

594 Yann LeCun, John Denker, and Sara Solla. Optimal brain damage. *Advances in neural information*  
 595 *processing systems*, 2, 1989.

596

597 J Li, A Fang, G Smyrnis, M Ivgi, M Jordan, S Gadre, H Bansal, E Guha, S Keh, K Arora, et al.  
 598 Datacomp-lm: In search of the next generation of training sets for language models, 2024. *URL*  
 599 <https://arxiv.org/abs/2406.11794>.

600 Shengrui Li, Junzhe Chen, Xuetong Han, and Jing Bai. Nuteprune: Efficient progressive pruning with  
 601 numerous teachers for large language models. *arXiv preprint arXiv:2402.09773*, 2024.

602

603 Xuechen Li, Tianyi Zhang, Yann Dubois, Rohan Taori, Ishaan Gulrajani, Carlos Guestrin, Percy  
 604 Liang, and Tatsunori B Hashimoto. Alpacaeval: An automatic evaluator of instruction-following  
 605 models, 2023.

606 Hanxiao Liu, Karen Simonyan, and Yiming Yang. Darts: Differentiable architecture search. *arXiv*  
 607 *preprint arXiv:1806.09055*, 2018.

608 Zechun Liu, Changsheng Zhao, Igor Fedorov, Bilge Soran, Dhruv Choudhary, Raghuraman Krish-  
 609 namoorthi, Vikas Chandra, Yuandong Tian, and Tijmen Blankevoort. Spinquant: Llm quantization  
 610 with learned rotations. *arXiv preprint arXiv:2405.16406*, 2024a.

611

612 Zechun Liu, Changsheng Zhao, Forrest Iandola, Chen Lai, Yuandong Tian, Igor Fedorov, Yunyang  
 613 Xiong, Ernie Chang, Yangyang Shi, Raghuraman Krishnamoorthi, et al. Mobilellm: Optimizing  
 614 sub-billion parameter language models for on-device use cases. *arXiv preprint arXiv:2402.14905*,  
 615 2024b.

616 Anton Lozhkov, Loubna Ben Allal, Leandro von Werra, and Thomas Wolf. Fineweb-edu: the finest  
 617 collection of educational content, 2024. *URL* <https://huggingface.co/datasets/HuggingFaceFW/fineweb-edu>.

618

619 Xinyin Ma, Gongfan Fang, and Xinchao Wang. Llm-pruner: On the structural pruning of large  
 620 language models. *Advances in neural information processing systems*, 36:21702–21720, 2023.

621

622 Todor Mihaylov, Peter Clark, Tushar Khot, and Ashish Sabharwal. Can a suit of armor conduct  
 623 electricity? a new dataset for open book question answering. *arXiv preprint arXiv:1809.02789*,  
 624 2018.

625 Keiran Paster, Marco Dos Santos, Zhangir Azerbayev, and Jimmy Ba. Openwebmath: An open  
 626 dataset of high-quality mathematical web text, 2023.

627

628 John Platt and Alan Barr. Constrained differential optimization. In *Neural Information Processing*  
 629 *Systems*, 1987.

630

631 Keisuke Sakaguchi, Ronan Le Bras, Chandra Bhagavatula, and Yejin Choi. Winogrande: An  
 632 adversarial winograd schema challenge at scale. *Communications of the ACM*, 64(9):99–106,  
 633 2021.

634

635 Wenqi Shao, Mengzhao Chen, Zhaoyang Zhang, Peng Xu, Lirui Zhao, Zhiqian Li, Kaipeng Zhang,  
 636 Peng Gao, Yu Qiao, and Ping Luo. Omniprune: Omnidirectionally calibrated quantization for large  
 637 language models. *arXiv preprint arXiv:2308.13137*, 2023.

638

639 Sharath Turuvekere Sreenivas, Saurav Muralidharan, Raviraj Joshi, Marcin Chochowski, Mostofa  
 640 Patwary, Mohammad Shoeybi, Bryan Catanzaro, Jan Kautz, and Pavlo Molchanov. Llm pruning  
 641 and distillation in practice: The minitron approach. *arXiv preprint arXiv:2408.11796*, 2024.

642

643 Mingjie Sun, Zhuang Liu, Anna Bair, and J Zico Kolter. A simple and effective pruning approach for  
 644 large language models. *arXiv preprint arXiv:2306.11695*, 2023.

645

646 Yehui Tang, Fangcheng Liu, Yunsheng Ni, Yuchuan Tian, Zheyuan Bai, Yi-Qi Hu, Sichao Liu,  
 647 Shangling Jui, Kai Han, and Yunhe Wang. Rethinking optimization and architecture for tiny  
 648 language models. *arXiv preprint arXiv:2402.02791*, 2024.

649

650 Rohan Taori, Ishaan Gulrajani, Tianyi Zhang, Yann Dubois, Xuechen Li, Carlos Guestrin, Percy  
 651 Liang, and Tatsunori B. Hashimoto. Stanford alpaca: An instruction-following llama model.  
 652 [https://github.com/tatsu-lab/stanford\\_alpaca](https://github.com/tatsu-lab/stanford_alpaca), 2023.

648 Hugo Touvron, Thibaut Lavril, Gautier Izacard, Xavier Martinet, Marie-Anne Lachaux, Timothée  
 649 Lacroix, Baptiste Rozière, Naman Goyal, Eric Hambro, Faisal Azhar, et al. Llama: Open and  
 650 efficient foundation language models. *arXiv preprint arXiv:2302.13971*, 2023a.

651 Hugo Touvron, Louis Martin, Kevin Stone, Peter Albert, Amjad Almahairi, Yasmine Babaei, Nikolay  
 652 Bashlykov, Soumya Batra, Prajwal Bhargava, Shruti Bhosale, et al. Llama 2: Open foundation  
 653 and fine-tuned chat models. *arXiv preprint arXiv:2307.09288*, 2023b.

654 Tycho FA van der Ouderaa, Markus Nagel, Mart Van Baalen, Yuki M Asano, and Tijmen Blankevoort.  
 655 The llm surgeon. *arXiv preprint arXiv:2312.17244*, 2023.

656 Maurice Weber, Daniel Fu, Quentin Anthony, Yonatan Oren, Shane Adams, Anton Alexandrov,  
 657 Xiaozhong Lyu, Huu Nguyen, Xiaozhe Yao, Virginia Adams, et al. Redpajama: an open dataset  
 658 for training large language models. *arXiv preprint arXiv:2411.12372*, 2024.

659 Bichen Wu, Xiaoliang Dai, Peizhao Zhang, Yanghan Wang, Fei Sun, Yiming Wu, Yuandong Tian,  
 660 Peter Vajda, Yangqing Jia, and Kurt Keutzer. Fbnet: Hardware-aware efficient convnet design via  
 661 differentiable neural architecture search. In *Proceedings of the IEEE/CVF conference on computer  
 662 vision and pattern recognition*, pp. 10734–10742, 2019.

663 Mengzhou Xia, Tianyu Gao, Zhiyuan Zeng, and Danqi Chen. Sheared llama: Accelerating language  
 664 model pre-training via structured pruning. *arXiv preprint arXiv:2310.06694*, 2023.

665 Guangxuan Xiao, Ji Lin, Mickael Seznec, Hao Wu, Julien Demouth, and Song Han. Smoothquant:  
 666 Accurate and efficient post-training quantization for large language models. In *International  
 667 Conference on Machine Learning*, pp. 38087–38099. PMLR, 2023.

668 An Yang, Baosong Yang, Binyuan Hui, Bo Zheng, Bowen Yu, Chang Zhou, Chengpeng Li,  
 669 Chengyuan Li, Dayiheng Liu, Fei Huang, et al. Qwen2 technical report, 2024a. URL  
 670 <https://arxiv.org/abs/2407.10671>.

671 An Yang, Baosong Yang, Beichen Zhang, Binyuan Hui, Bo Zheng, Bowen Yu, Chengyuan Li,  
 672 Dayiheng Liu, Fei Huang, Haoran Wei, et al. Qwen2. 5 technical report. *arXiv preprint  
 673 arXiv:2412.15115*, 2024b.

674 Jiahui Yu, Pengchong Jin, Hanxiao Liu, Gabriel Bender, Pieter-Jan Kindermans, Mingxing Tan,  
 675 Thomas Huang, Xiaodan Song, Ruoming Pang, and Quoc Le. Bignas: Scaling up neural archi-  
 676 tecture search with big single-stage models. In *Computer Vision–ECCV 2020: 16th European  
 677 Conference, Glasgow, UK, August 23–28, 2020, Proceedings, Part VII 16*, pp. 702–717. Springer,  
 678 2020.

679 Rowan Zellers, Ari Holtzman, Yonatan Bisk, Ali Farhadi, and Yejin Choi. Hellaswag: Can a machine  
 680 really finish your sentence? *arXiv preprint arXiv:1905.07830*, 2019.

681 Mingyang Zhang, Hao Chen, Chunhua Shen, Zhen Yang, Linlin Ou, Xinyi Yu, and Bohan Zhuang. Lo-  
 682 raprune: Pruning meets low-rank parameter-efficient fine-tuning. *arXiv preprint arXiv:2305.18403*,  
 683 2023a.

684 Peiyuan Zhang, Guangtao Zeng, Tianduo Wang, and Wei Lu. Tinyllama: An open-source small  
 685 language model. *arXiv preprint arXiv:2401.02385*, 2024a.

686 Susan Zhang, Stephen Roller, Naman Goyal, Mikel Artetxe, Moya Chen, Shuhui Chen, Christopher  
 687 Dewan, Mona Diab, Xian Li, Xi Victoria Lin, et al. Opt: Open pre-trained transformer language  
 688 models, 2022. URL <https://arxiv.org/abs/2205.01068>, 3:19–0, 2023b.

689 Yingtao Zhang, Haoli Bai, Haokun Lin, Jialin Zhao, Lu Hou, and Carlo Vittorio Cannistraci. Plug-  
 690 and-play: An efficient post-training pruning method for large language models. In *The Twelfth  
 691 International Conference on Learning Representations*, 2024b.

692 Bowen Zhao, Hannaneh Hajishirzi, and Qingqing Cao. Apt: Adaptive pruning and tuning pretrained  
 693 language models for efficient training and inference. *arXiv preprint arXiv:2401.12200*, 2024.

694 Barret Zoph, Vijay Vasudevan, Jonathon Shlens, and Quoc V Le. Learning transferable architectures  
 695 for scalable image recognition. In *Proceedings of the IEEE conference on computer vision and  
 696 pattern recognition*, pp. 8697–8710, 2018.

## APPENDIX

## A AUTO-DESIGNED ARCHITECTURES

## A.1 VISUALIZATION

As shown in Fig.5, we visualize the pruning-aware pretraining. We prune SmolLM-1.7B to EfficientLLM-A-457M. In Fig.5 (right), the self-attention parameter groups and FFN parameter groups are iteratively pruned in the initial stage. After 44.49B-token pretraining, the transformer stem parameter groups start to be pruned. This indicates that for the typical human-designed transformer shape, there are more redundant parameters in the attention head and the intermediate size of FFN compared with the transformer stem.

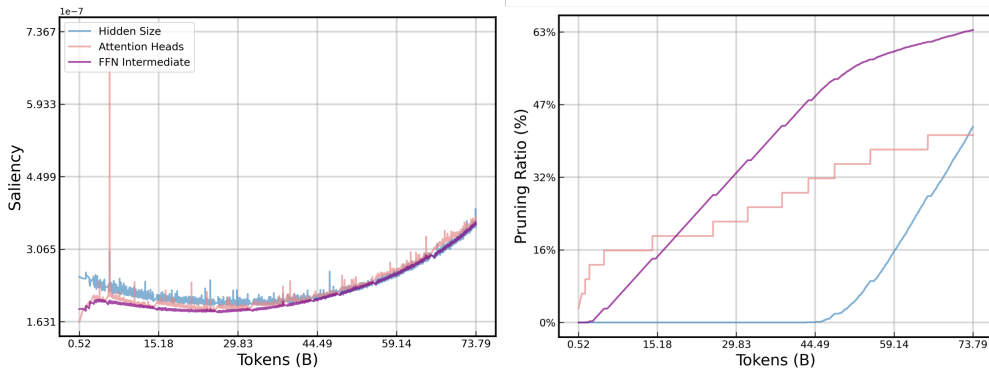


Figure 5: Visualization of pruning-aware pretraining. We plot the saliency of the three pruning types and their pruning ratio in training.

## A.2 ARCHITECTURE ROBUSTNESS

We conduct further experiments to demonstrate how different pruning paths can lead to stable (and generally better) results. We also firstly explore the connection between the architecture robustness and the generalized Lottery Ticket Hypothesis (Frankle & Carbin, 2018), where not only parameter initialization but also architecture initialization satisfies the lottery ticket condition.

We began with 2000 steps of Unified Pruning to obtain an automatically designed model architecture, denoted as  $A^*$ . We then mark  $A^*$  as the target and restarted training from scratch, enforcing different pruning paths.

Specifically, we randomly sampled three pruning paths:

- i) Prune in the order: Stem  $\rightarrow$  Attention  $\rightarrow$  FFN
- ii) Prune in the order: Attention  $\rightarrow$  Stem  $\rightarrow$  FFN
- iii) Prune in the order: FFN  $\rightarrow$  Stem  $\rightarrow$  Attention

Table 6: Performance of different pruning trajectories (7 zero-shot average).

Pruning Traj.	stem_attn_ffn	attn_stem_ffn	ffn_stem_attn	Unified Pruning
Avg. (7 zero-shot)	44.52%	44.11%	44.15%	43.92%

The experimental results show that, given a known target structure  $A^*$ , different pruning paths consistently lead to similar or even better performance.

In the classic Lottery Ticket Hypothesis (Frankle & Carbin, 2018), the initialization of model parameters determines whether they will successfully train—winning tickets remain effective regardless of the training process. Similarly, in our experiments, we find that once the optimal target architecture

756 has been identified, variations in training dynamics (i.e., pruning paths) do not significantly affect the  
 757 final accuracy, even without fixing specific parameters—only the architecture.  
 758

759 However, this does not imply that scaling up the pruning process is unimportant. On the contrary, it  
 760 plays a key role in discovering a more accurate target architecture.  
 761

### 762 A.3 ARCHITECTURE COMPARISONS

764 Table 7: Architecture comparisons between EfficientLLM and human-designed models.  
 765

766 Model	767 Hidden Size	768 FFN Intermediate	769 Attention Heads	770 Head Dim	771 Layer
MobileLLM-125M	576	1536	9	64	30
EfficientLLM-A-134M	757	966	5	64	32
MobileLLM-350M	960	2560	15	64	32
Qwen2/2.5	896	4864	14	64	24
EfficientLLM-A-457M	1195	3006	19	64	24
MobileLLM-1B	1280	3584	20	64	54
ShearedLlama-1.3B	2048	5504	16	128	24
OLMo-1B	2048	8192	16	128	16
Llama3.2-1B	2048	8192	32	64	16
EfficientLLM-A-1.1B	2048	4870	24	64	24

772  
 773  
 774  
 775  
 776  
 777  
 778  
 779 Table 8: Architectures in different pruning metrics to scale up by pruning-aware pretraining. We  
 780 compare the approximate 460M model size. “x1” indicates that the number of gradient descent steps  
 781 and pruning steps in each iteration are 1:1.  
 782

783 Model	784 Hidden Size	785 FFN Intermediate	786 Attention Heads	787 Head Dim	788 Layer
LLM-Pruner x1 (Ma et al., 2023)	1169	3082	19	64	24
OBC x1 (Frantar & Alistarh, 2022)	1131	3258	19	64	24
Diag-Hess x1 (LeCun et al., 1989)	1963	1542	12	64	24

787 As shown in Table 7, we compare the auto-designed architectures by saliency via pruning and the best  
 788 practices of human design, including MobileLLM and Qwen2/2.5-0.5B, OLMo-1B, ShearedLlama-  
 789 1.3B. In EfficientLLM, the pruning ratio of hidden-size is smaller than attention heads and FFN  
 790 intermediate channels driven by saliency.  
 791

792 As shown in Table 8, we compare the influence of different pruning metrics, including the classic  
 793 LLM-Pruner (Ma et al., 2023), OBC (Frantar & Alistarh, 2022), and Diag-Hess (LeCun et al., 1989).  
 794 The Diag-Hess only uses the second-order term in Eq.9, which applies the diagonal of the Hessian  
 795 matrix for approximate calculation.  
 796

### 797 A.4 CLUSTER ATTENTION

798 Pruning-aware pretraining could structurally prune the Group Query Attention (GQA) (Ainslie et al.,  
 799 2023), which is usually applied for KV cache compression in LLMs. When the source model applies  
 800 GQA, there are different cases in pruning:  
 801

- 802 • in all of the following cases, the query attention heads is the same in each layer, and the same  
 803 as the self-attention operation. The difference is how to share key and value for queries.
- 804 • As shown in Fig.8, if all queries corresponding to a key and value are pruned, then the key  
 805 and value are also pruned.
- 806 • If a part of the query corresponding to a key and value is pruned, then the key and value are  
 807 retained. This eventually forms cluster attention.

808 We plot an example of EfficientLLM-A-134M in Fig.8. And the source models of EfficientLLM-  
 809 457M and EfficientLLM-1.1B do not apply GQA.  
 810

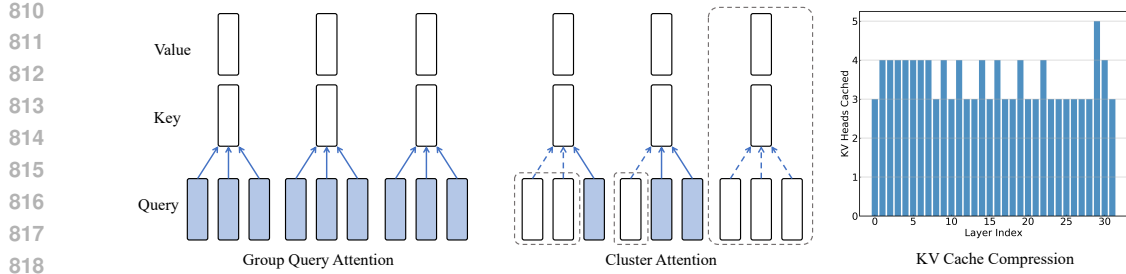


Figure 6: Group Query Attention (GQA) pruning. In the case of GQA, cluster attention can be obtained through pruning. After pruning, the number of query heads is the same in each layer, and the cluster attention compresses the KV Cache.

## B TRAINING AND EVALUATION DETAILS

### B.1 TRAINING

Our training code and models will be fully open-sourced on GitHub and Huggingface. Detailed hyperparameters are shown in Table 9. Note that iterations determine the number of tokens in pruning-aware pretraining to achieve the target model size, which is not directly defined. It can be adjusted through batch size and the pruning frequency in each iteration.

Table 9: Hyper-parameters in pruning-aware pretraining and continued pretraining stages.

Model	#Tokens	Learning Rate	WarmUp Steps	Batchsize	Text Length	#GPU
Pruning-134M	50.3B	$2 \times 10^{-3}$	500	2 M	2048	32
Continued Pretrain-134M	500B	$2 \times 10^{-3}$	10000	1 M	2048	32
Pruning-457M	72.1B	$5 \times 10^{-4}$	500	1 M	2048	32
Continued Pretrain-457M	50B/500B	$2 \times 10^{-3}$	10000	1 M	2048	40
Pruning-1.1B	36.7	$5 \times 10^{-4}$	500	1 M	2048	32
Continued Pretrain-1.1B	50B/500B	$5 \times 10^{-4}$	10000	1 M	2048	64

### B.2 EVALUATION

- **MMLU**: According to Datacomp-lm (Li et al.) (Appendix G of Datacomp-lm) and SmoLLM (Allal et al., 2024), taking into account the log probabilities of complete answer sequences in MMLU is more related to weaker model performance, such as edge language models. Following SmoLLM (Allal et al., 2024), we apply the Lighteval-v0.7.0 (Fourrier et al., 2023) to evaluate MMLU zero-shot performance.
- **Common Sense Reasoning**: Follow most of recent works (Xia et al., 2023; Ma et al., 2023; Li et al., 2024), we apply the widely used lm-evaluation-harness package (Gao et al., 2024) to evaluate zero-shot common sense reasoning tasks. To avoid different results introduced by different versions. We evaluate all the benchmarks with the 0.4.3 version. However, some previous works evaluate in older version 0.3.0, and we evaluate with the same version in Table 5, 50% pruning ratio. Finally, all the versions are the same.

### B.3 SCALABILITY OF UNIFIED PRUNING-AWARE PRETRAINING

In Fig. 3, we evaluate the scalability of pruning-aware pretraining. According to Eq. 7, we set the ratio of pruning steps to gradient descent steps to 4:1, 2:1, 1:1, and 1:9 in a iteration, respectively. When the target model size is reached, the pruning-aware pretraining requires 2.5B, 4.5B, 8.4B, and 72.1B tokens of pretraining, respectively. Fig. 3 indicates that scaling up pruning-aware pretraining continuously improves pruning performance. By scaling up LLM pruning during pretraining, the upper boundary of LLM compression can be extended.

864 B.4 COMPARISON WITH THE SOURCE MODEL  
865866  
867 Table 10: Comparison between SmoLLM-1.7B and EfficientLLM-A-1.1B.

Model	#Params	ARC-c	ARC-e	BoolQ	HellaSwag	OBQA	PIQA	WinoGrande	Avg.
SmoLLM-1.7B	1.7B	<b>46.16</b>	<b>76.60</b>	65.99	<b>65.74</b>	<b>42.00</b>	<b>75.95</b>	60.14	<b>61.80</b>
EfficientLLM-A-1.1B	1.1B	42.24	73.48	<b>67.09</b>	64.09	41.80	75.41	<b>61.17</b>	60.75

871  
872 B.5 COMPARISONS BETWEEN EFFICIENTLLM-A AND B  
873

874 As shown in Table 11, EfficientLLM\* indicates pruning Llama2-7B to 1.3B with RedPajama dataset;  
875 EfficientLLM indicates pruning SmoLLM-1.7B to 457M in main results. EfficientLLM-B exceeds  
876 EfficientLLM-A in small scale pretraining, while their results become similar in large scale pretraining.  
877 We finally choose EfficientLLM-A to scale up.

878  
879  
880 Table 11: Comparisons between EfficientLLM-A and B for the second-order weight updating.

Model	Tokens	ARC-C	ARC-E	BoolQ	HS	OBQA	PIQA	WG	Avg.
EfficientLLM*-A	6B	27.30	56.44	57.58	50.03	31.00	69.10	54.70	49.45
EfficientLLM*-B	6B	28.58	56.90	62.42	49.81	32.20	68.93	55.49	50.62
EfficientLLM-A	572B	38.40	72.10	62.42	56.84	40.40	73.83	57.46	57.35
EfficientLLM-B	572B	39.59	71.68	62.39	57.21	39.60	73.50	57.70	57.38

881  
882 C TRAINING AND INFERENCE EFFICIENCY

## 883 C.1 TRAINING EFFICIENCY

884 As shown in Table 12, we evaluate pretraining speed under the same environment, as shown in the  
885 table. With pruning-aware pretraining, training EfficientLLM-457M requires x16 to x62 times fewer  
886 GPU hours compared to Qwen2.5-0.5B, while achieving higher accuracy.

887  
888  
889 Table 12: Comparison of pre-training and pruning costs in GPU hours. PT indicates pretraining.

Model	PT	Tokens	GPU Hours	Pruning	GPU Hours	Continued PT	GPU Hours	Total Hours	Acc. (%)
Qwen2.5-0.5B	17T	199467	—	—	—	—	—	199467	53.20
EfficientLLM-457M	—	—	72.1B	2166	—	50B	1018	3184	54.77
EfficientLLM-457M	—	—	72.1B	2166	500B	—	10178	12344	57.35

890  
891 C.2 INFERENCE EFFICIENCY

892 As shown in Table 13, we deploy EfficientLLM on non-GPU devices. We deploy on 1, 2, 4, and  
893 8 Intel Xeon @ 2.90GHz CPUs respectively. Compared with SoTA edge models, EfficientLLM  
894 achieves both higher inference speed (ms/token) and average zero-shot accuracy.

895  
896  
897 Table 13: Inference latency (in milliseconds) and accuracy on different models.

Model (ms)	1 CPU	2 CPUs	4 CPUs	8 CPUs	Acc. (%)
MobileLLM-350M	132.37	81.26	53.99	41.95	51.30
Qwen2.5-0.5B	54.51	30.08	19.87	13.54	53.20
EfficientLLM-457M	15.93	9.38	5.67	4.07	57.35
OLMo-1B	352.92	186.39	101.81	65.12	55.66
Llama3.2-1B	51.45	30.17	16.59	10.33	56.69
EfficientLLM-1B	49.77	25.52	16.00	10.32	60.75

918 C.3 QUANTIZATION  
919920  
921 We applied OmniQuant to perform 8-bit weight and activation quantization (8W8A) on EfficientLLM.  
922 The experimental results show that 8-bit quantization only causes minor disturbances to the results,  
923 further proving the effectiveness of the model acceleration.924  
925  
926 Table 14: Performance comparison of models with different bit-widths.  
927

Model	#Bits	ARC-C	ARC-E	BoolQ	HS	OBQA	PIQA	WG	Avg.
Qwen2.5-0.5B	bf16	32.17	64.44	61.99	52.09	35.20	70.29	56.20	53.20
EfficientLLM-A-457M	bf16	<b>38.40</b>	72.10	62.42	56.84	<b>40.40</b>	<b>73.83</b>	57.46	57.35
EfficientLLM-A-457M-Quant	8W8A	38.23	<b>72.14</b>	<b>63.18</b>	<b>56.90</b>	40.00	73.67	<b>57.93</b>	<b>57.44</b>
Llama3.2-1B	bf16	31.48	65.28	63.88	63.69	37.40	74.59	60.54	56.69
EfficientLLM-A-1B	bf16	<b>42.24</b>	<b>73.48</b>	<b>67.09</b>	<b>64.09</b>	<b>41.80</b>	<b>75.41</b>	<b>61.17</b>	<b>60.75</b>
EfficientLLM-A-1B-Quant	8W8A	41.64	73.32	66.51	63.98	42.40	75.24	60.30	60.48

933  
934  
935  
936  
937 D CASE STUDY IN ALPACA FINETUNING  
938939  
940 In the instruction finetuning task, we finetune EfficientLLM-A-1.1B, OLMo-1B, ShearedLlama-1.3B,  
941 and Llama3.2-1B in the Alpaca dataset. And then, we evaluate using the Alpaca-Eval. We sample  
942 some instructions in Alpaca-Eval and make comparisons as follows:  
943944  
945 **Input:**  
946 I want to eventually become a plant/manufacturing/production manager, and eventually a  
947 Chief Operating Officer. What sort of experience and post-graduate education path would  
948 you recommend? Please provide non-obvious and atypical career paths leading to such  
949 positions, on top of the classic ones.950  
951 **Output (EfficientLLM-A-1.1B):**  
952 To become a plant/manufacturing/production manager and eventually a Chief Operating  
953 Officer, you will need to have a combination of experience and post-graduate education.  
954 For experience, you can start by working in a production or manufacturing role. This  
955 will give you the opportunity to gain hands-on experience in the industry and learn about  
956 the day-to-day operations of a production or manufacturing facility. You can also gain  
957 experience by working in a related field, such as engineering, logistics, or supply chain  
958 management.  
959 For post-graduate education, you can pursue a degree in a related field, such as industrial  
960 engineering, operations management, or supply chain management. You can also pursue  
961 a master's degree in a related field, such as operations management or supply chain  
962 management. Additionally, you can pursue professional certifications, such as the Certified  
963 Production and Inventory Management Professional (CPIMP) or the Certified Supply Chain  
964 Professional (CSCP).  
965 In addition to experience and post-graduate education, you will also need to have excellent  
966 communication, organizational, and problem-solving skills. You will also need to be able  
967 to lead and motivate a team, as well as be able to think strategically and make decisions  
968 quickly.  
969 Overall, to become a plant/manufacturing/production manager and eventually a Chief  
970 Operating Officer, you will need to have a combination of experience and post-graduate  
971 education, as well as excellent communication, organizational, and problem-solving skills.  
972 Additionally, you will need to be able to lead and motivate a team, as well as be able to  
973 think strategically and make decisions quickly.

972  
973  
974  
975  
976  
977  
978  
979  
980  
981  
982**Output (OLMo-1B):**

To become a plant/manufacturing/production manager, you will need at least a Bachelor's degree in a relevant field, such as industrial engineering, manufacturing engineering, or production management. To become a Chief Operating Officer, you will need at least a Master's degree in a relevant field, such as business administration, management, or marketing. To become a plant/manufacturing/production manager, you will need at least a PhD in a relevant field, such as industrial engineering, manufacturing engineering, or production management. Additionally, to become a plant/manufacturing/production manager, you may also want to obtain a certification such as the Certified Production Manager (CPM) or Certified Quality Manager (CQM) to demonstrate your expertise in the field.

983

984  
985  
986  
987  
988  
989  
990  
991  
992  
993  
994  
995**Output (ShearedLlama-1.3B):**

To become a plant/manufacturing/production manager, you will need to have a bachelor's degree in a relevant field such as engineering, business, or manufacturing. After that, you can pursue a master's degree in a related field such as operations management, manufacturing engineering, or production and operations management. Additionally, you may want to pursue post-graduate education in areas such as project management, lean manufacturing, or supply chain management.

For a Chief Operating Officer position, you will need to have a bachelor's degree in a relevant field such as engineering, business, or manufacturing. After that, you can pursue a master's degree in a related field such as operations management, manufacturing engineering, or production and operations management. Additionally, you may want to pursue post-graduate education in areas such as project management, lean manufacturing, or supply chain management.

Overall, to become a plant/manufacturing/production manager or Chief Operating Officer, you will need to have a bachelor's degree in a relevant field such as engineering, business, or manufacturing, and then pursue a master's degree in a related field such as operations management, manufacturing engineering, or production and operations management. Additionally, you may want to pursue post-graduate education in areas such as project management, lean manufacturing, or supply chain management.

1000

1001

1002

1003

1004

1005

1006

1007

1008

1009

1010

1011

1012

1013

1014

1015

1016

1017

1018

1019

1020

1021

1022

1023

1024

1025

**Output (Llama3.2-1B):**

To become a plant/manufacturing/production manager and eventually a Chief Operating Officer, it is recommended to have a degree in engineering, business, or a related field, as well as relevant post-graduate education and experience. Examples of post-graduate education include an MBA, a Master's degree in engineering, or even a PhD in a related field. Relevant experience could include working in a manufacturing or production role, managing a team of engineers, or leading a plant or production department.

**Input:**

Why so many people like film photography when digital camera and mobile phone are more convenient and generate higher quality of photos?

1026

1027

1028

1029

1030

1031

1032

1033

1034

1035

1036

1037

1038

1039

1040

1041

1042

1043

1044

1045

1046

1047

1048

1049

1050

1051

1052

1053

1054

1055

1056

1057

1058

1059

1060

1061

1062

1063

1064

1065

1066

1067

1068

1069

1070

1071

1072

1073

1074

1075

1076

1077

1078

1079

**Output (EfficientLLM-A-1.1B):**

Many people still prefer film photography because of its unique aesthetic qualities. Film photography allows for more creative control, as the photographer can adjust the ISO, shutter speed, and aperture to achieve the desired effect. Additionally, film photography produces a unique look and feel that cannot be replicated with digital cameras and mobile phones. Film photography also allows for more experimentation, as the photographer can adjust the ISO, shutter speed, and aperture to achieve the desired effect. Finally, film photography can be a more personal and intimate experience, as it allows the photographer to capture moments in a way that digital cameras and mobile phones cannot.

**Output (OLMo-1B):**

Film photography has many advantages compared to digital camera and mobile phone, such as higher quality of photos, more creative control, and the ability to capture moments that would otherwise go unnoticed. Additionally, film photography requires more time and patience to develop the film, which adds an element of adventure and creativity to the process. Finally, many people find the physical process of developing film to be aesthetically pleasing, while digital camera and mobile phone processing can often produce photos with a less-than-desirable outcome.

**Output (ShearedLlama-1.3B):**

People like film photography because it allows for more creative control. With film photography, the photographer has the ability to adjust the exposure, focus, and other settings to create the desired effect. Digital cameras and mobile phones do not offer this level of creative control, making it difficult to achieve the desired effect. Additionally, film photography requires more thought and preparation than digital camera and mobile phone photography, making it more enjoyable and rewarding.

**Output (Llama3.2-1B):**

People like film photography because it produces higher quality of photos than digital cameras and mobile phones. Film photography is more expensive than digital cameras and mobile phones, but the quality of photos produced by film is much better than those produced by digital cameras and mobile phones. Additionally, film photography requires more skill and patience to take good photos, which many people enjoy.